NASA/TM—2008-215156 AIAA–2008–312

# Vibration Analysis of the Space Shuttle External Tank Cable Tray Flight Data With and Without PAL Ramp

*Bruce E. Walker*
*Channel Islands Acoustics, Camarillo, California*

*Jayanta Panda*
*Ohio Aerospace Institute, Brook Park, Ohio*

*Daniel L. Sutliff*
*Glenn Research Center, Cleveland, Ohio*

March 2008

# NASA STI Program . . . in Profile

Since its founding, NASA has been dedicated to the advancement of aeronautics and space science. The NASA Scientific and Technical Information (STI) program plays a key part in helping NASA maintain this important role.

The NASA STI Program operates under the auspices of the Agency Chief Information Officer. It collects, organizes, provides for archiving, and disseminates NASA's STI. The NASA STI program provides access to the NASA Aeronautics and Space Database and its public interface, the NASA Technical Reports Server, thus providing one of the largest collections of aeronautical and space science STI in the world. Results are published in both non-NASA channels and by NASA in the NASA STI Report Series, which includes the following report types:

- TECHNICAL PUBLICATION. Reports of completed research or a major significant phase of research that present the results of NASA programs and include extensive data or theoretical analysis. Includes compilations of significant scientific and technical data and information deemed to be of continuing reference value. NASA counterpart of peer-reviewed formal professional papers but has less stringent limitations on manuscript length and extent of graphic presentations.

- TECHNICAL MEMORANDUM. Scientific and technical findings that are preliminary or of specialized interest, e.g., quick release reports, working papers, and bibliographies that contain minimal annotation. Does not contain extensive analysis.

- CONTRACTOR REPORT. Scientific and technical findings by NASA-sponsored contractors and grantees.

- CONFERENCE PUBLICATION. Collected papers from scientific and technical conferences, symposia, seminars, or other meetings sponsored or cosponsored by NASA.

- SPECIAL PUBLICATION. Scientific, technical, or historical information from NASA programs, projects, and missions, often concerned with subjects having substantial public interest.

- TECHNICAL TRANSLATION. English-language translations of foreign scientific and technical material pertinent to NASA's mission.

Specialized services also include creating custom thesauri, building customized databases, organizing and publishing research results.

For more information about the NASA STI program, see the following:

- Access the NASA STI program home page at *http://www.sti.nasa.gov*

- E-mail your question via the Internet to *help@sti.nasa.gov*

- Fax your question to the NASA STI Help Desk at 301–621–0134

- Telephone the NASA STI Help Desk at 301–621–0390

- Write to:
  NASA Center for AeroSpace Information (CASI)
  7115 Standard Drive
  Hanover, MD 21076–1320

NASA/TM—2008-215156 AIAA–2008–312

# Vibration Analysis of the Space Shuttle External Tank Cable Tray Flight Data With and Without PAL Ramp

*Bruce E. Walker*
*Channel Islands Acoustics, Camarillo, California*

*Jayanta Panda*
*Ohio Aerospace Institute, Brook Park, Ohio*

*Daniel L. Sutliff*
*Glenn Research Center, Cleveland, Ohio*

Prepared for the
46th Aerospace Sciences Meeting and Exhibit
sponsored by the American Institute of Aeronautics and Astronautics
Reno, Nevada, January 7–10, 2008

National Aeronautics and
Space Administration

Glenn Research Center
Cleveland, Ohio 44135

March 2008

## Acknowledgments

The authors wish to thank the NASA Engineering Safety Center (NESC) for supporting this work.

*Level of Review*: This material has been technically reviewed by technical management.

Available from

NASA Center for Aerospace Information
7115 Standard Drive
Hanover, MD 21076–1320

National Technical Information Service
5285 Port Royal Road
Springfield, VA 22161

Available electronically at http://gltrs.grc.nasa.gov

# Vibration Analysis of the Space Shuttle External Tank Cable Tray Flight Data With and Without PAL Ramp

Bruce E. Walker
Channel Islands Acoustics
Camarillo, California 93010

Jayanta Panda
Ohio Aerospace Institute
Brook Park, Ohio 44142

Daniel L. Sutliff
National Aeronautics and Space Administration
Glenn Research Center
Cleveland, Ohio 44135

## Abstract

External Tank Cable Tray vibration data for three successive Space Shuttle flights were analyzed to assess response to buffet and the effect of removal of the Protuberance Air Loads (PAL) ramp. Waveform integration, spectral analysis, cross-correlation analysis and wavelet analysis were employed to estimate vibration modes and temporal development of vibration motion from a sparse array of accelerometers and an on-board system that acquired 16 channels of data for approximately the first 2 min of each flight. The flight data indicated that PAL ramp removal had minimal effect on the fluctuating loads on the cable tray. The measured vibration frequencies and modes agreed well with predicted structural response.

## Nomenclature

| | |
|---|---|
| $a$ | instantaneous (time dependent) value of measured accelerometer signal |
| $v$ | instantaneous (time dependent) value of time-integrated accelerometer signal (velocity) |
| $x$ | instantaneous (time dependent) value of double time-integrated accelerometer signal (displacement) |
| $t$ | elapsed time |
| $A$-$E$ | measurement system start-up transient decay parameters |
| $\Delta$ | process of removing linear signal trends test data |
| $\Psi$ | continuous wavelet transformation |
| $\psi$ | complex Morlet wavelet function |
| $F_b$, $F_c$ | Morlet wavelet function frequency parameters |
| $S$ | scaled factor for wavelet transformation |
| T | time interval between data samples |
| $p$-$p$ | peak to peak amplitude designation |
| EDAS | Enhanced Data Acquisition System |
| ET | External Tank |
| DFI | Development Flight Information |
| HOSC | Huntsville Operations Support Center |
| $LO_2$ | Liquid Oxygen |
| $LH_2$ | Liquid Hydrogen |
| MSID | Measurement Station Identifcation |
| NESC | NASA Engineering Safety Center |
| NTS | Not to Scale |
| PAL | Protuberance Aerodynamic Load |
| RTF | Return to Flight |
| SRB | Solid Rocket Booster |

# I. Introduction

In the wake of the Columbia tragedy, a priority was established to eliminate foam elements from various regions on the Space Shuttle External Fuel Tank. One such region was the Protuberance Aerodynamics Load ramps located beside portions of the Cable Trays that run from near the top to near the bottom of the ET as shown in figures 1 and 2. Prior to Return to Flight, computational modeling, ground vibration testing (ref. 1), and component wind tunnel testing (ref. 2) was accomplished to assess the effect of removing these ramps on the dynamic loads on the protuberances. A Development Flight Information study was undertaken to verify the in-flight loads on three shuttle flights to assess the effect of removing these ramps on the structural integrity of the protuberances. Specifically, a sparse array of accelerometers was installed within cable trays near the PAL ramp locations and vibration response was recorded for three Shuttle flights, one with PAL ramps present and two with the ramps removed.

The original intention of the PAL ramp was to protect ET protuberances from significant cross-flows. Various earlier flow-visualization images showed that during the transonic flight regime shock waves emanating from the SRB and the Orbiter nose-cone impinged upon the External Tank and created potential for the strong cross-flow velocity. When the PAL ramp was to be removed the protuberances were to face the cross-flow once again. Various analysis, ground vibration testing and component wind tunnel testing indicated that the aerodynamic load on the protuberances may be small compared to various other sources of steady and unsteady load, most notably, the transmitted vibration through the mounting brackets (Ice/Frost ramps) and thermal load.

True flight environment is difficult to establish by any ground-testing effort. Therefore, the DFI instruments were used to provide a final check on the structural integrity of the protuberances. In addition to the Cable Tray, other protuberances of concern were the gaseous Oxygen pressurization line, the gaseous Hydrogen pressurization line and the Feed-line. Out of all these elements only the Cable Tray allows for easy installation of the DFI sensors.

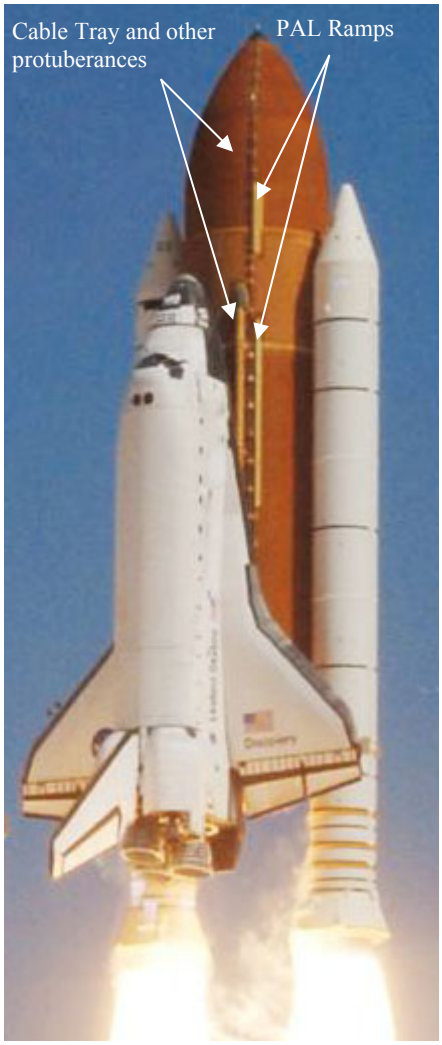


Figure 1.—Location of the PAL ramp and External Tank protuberances on the Space Shuttle.

In order to validate predictions and wind tunnel tests of fluctuating aerodynamic loads on these protuberances, segments of the cable trays near PAL ramp locations in the $LO_2$ and $LH_2$ tank areas were instrumented with accelerometers. Vibration data from these sensors were recorded for approximately 2 min in each of three shuttle flights (STS-114, STS-121, and STS-115). Cable tray cross sections are shown schematically in figure 3. The presence/absence of the PAL ramps for these three flights is shown in table I.

Because shuttle flight data is comparatively rare, multiple teams, including NESC, United Space Alliance/Boeing, NASA Langley, and Lockheed-Martin, conducted in-depth analyses of the acceleration data and potential structural load implications.

The present report is part of the NESC effort, which used spectrographic, cross-correlation, wavelet transform and waveform integration techniques to assess the vibration responses of the trays as a function of time and overall aerodynamic loads. In this paper, we will present an overview of the measurement data, discussion of the analysis methods and a summary of the results.


(a)

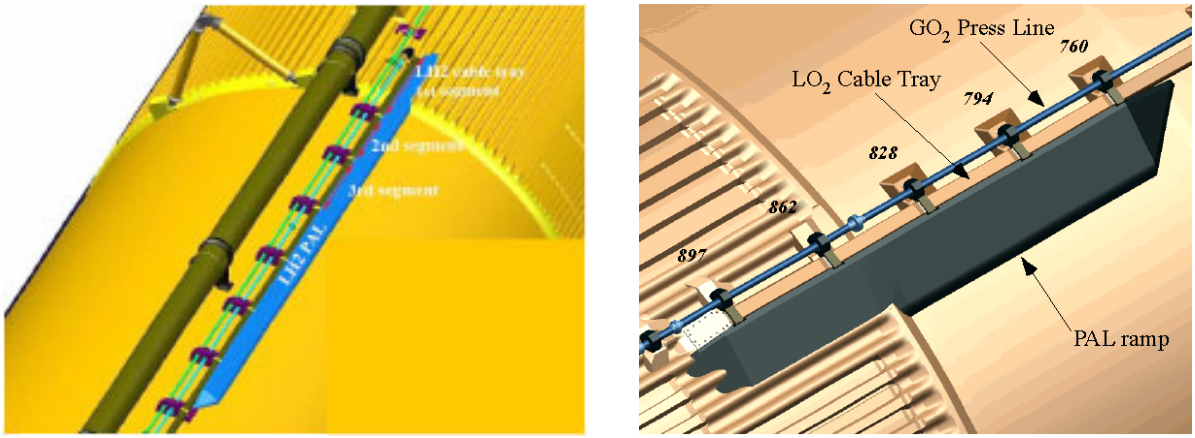


(b)

Figure 2.—(a) Photo of External Tank with close-up of PAL ramps. (b). Schematic of Cable Tray Instrumentation Locations near PAL ramps.

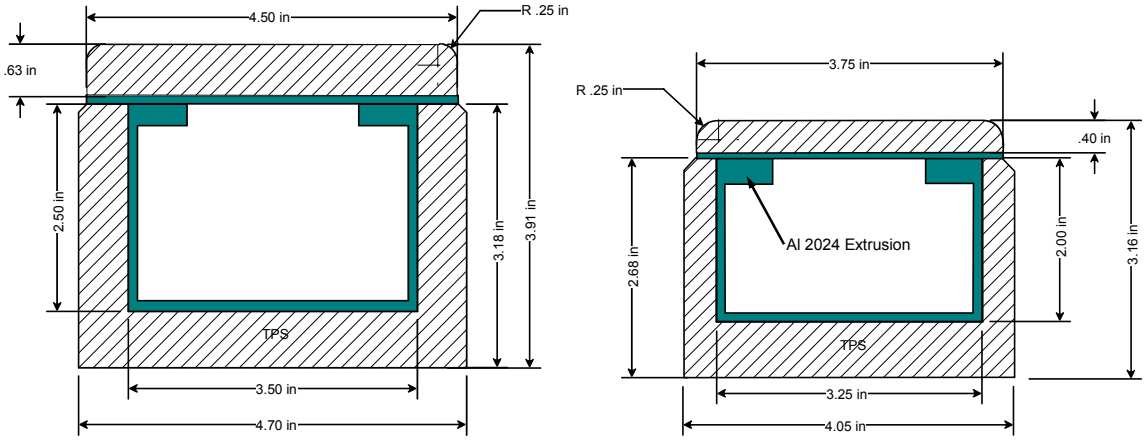


Figure 3.—Cross Sections of $LH_2$ and $LO_2$ Cable Trays.

TABLE I.—SHUTTLE FLIGHT PAL RAMP CONFIGURATION

| Flight | STS-114 | STS-121 | STS-115 |
|---|---|---|---|
| PAL ramps | On | Off | Off |
| Accelerometers | $LO_2$ only | $LO_2$ and $LH_2$ | $LO_2$ and $LH_2$ |

TABLE II.—CABLE TRAY ACCELEROMETER DESIGNATIONS AND LOCATIONS. ALSO INDICATED ARE EXTENTS OF PAL RAMPS, PRESENT IN STS-114 AND REMOVED FROM STS-121 AND STS-115

| MSID | Location | Measurement direction | Flight |
|---|---|---|---|
| $LO_2$ ramp start | Approx 760 | | |
| T08D9067A | $LO_2$ C/T BIAXIAL Xt = 845 | Radial | 114/121/115 |
| T08D9068A | $LO_2$ C/T BIAXIAL Xt = 845 | Tangential | 114/121/115 |
| T08D9069A | $LO_2$ C/T UNIAXIAL Xt = 845 | Radial | 114/121/115 |
| T08D9070A | $LO_2$ C/T UNIAXIAL Xt = 828 | Radial | 114/121/115 |
| T08D9075A | $LO_2$ C/T UNIAXIAL Xt = 860 | Radial | 114/121/115 |
| $LO_2$ ramp end | Approx 898 | | |
| | | | |
| $LH_2$ ramp start | Approx 1082 | | |
| T08D9091A | $LH_2$ C/T UNIAXIAL Xt = 1115 | Radial | - /121/115 |
| T08D9092A | $LH_2$ C/T UNIAXIAL Xt = 1116 | Radial | - /121/115 |
| T08D9093A | $LH_2$ C/T UNIAXIAL Xt = 1156 | Radial | - /121/115 |
| T08D9094A | $LH_2$ C/T UNIAXIAL Xt = 1176 | Radial | - /121/115 |
| T08D9095A | $LH_2$ C/T UNIAXIAL Xt = 1203 | Radial | - / - /115 |
| T08D9096A | $LH_2$ C/T UNIAXIAL Xt = 1235 | Radial | - / - /115 |
| T08D9097A | $LH_2$ C/T UNIAXIAL Xt = 1236 | Radial | - / - /115 |
| T08D9098A | $LH_2$ C/T BIAXIAL Xt = 1177 | Radial | - / - /115 |
| T08D9099A | $LH_2$ C/T BIAXIAL Xt = 1177 | Tangential | - /121/115 |
| $LH_2$ ramp end | Approx 1529 | | |

The sparse array of accelerometers was deployed along the cable trays in a distribution intended to provide end and mid-point data so that low-order longitudinal bending modes could be evaluated. In addition, at some locations radial and tangential acceleration sensors were collocated for evaluation of two-dimensional vibration patterns. At other locations, pairs of accelerometers were collocated axially but spaced tangentially to distinguish between radial and torsional vibration response. These positions are delineated, with the locations of PAL ramps, in table II.

# II. Data Acquisition

As outlined above, data was provided from a sparse array of one and two-axis accelerometers, distributed on the cable trays as shown schematically in figures 4 and 5. A typical installation photo is shown in figure 6. The basic concept was to provide signals for radial motion at the ends and near mid-span of each tray section, and in addition to provide tangential and/or torsional motion sensing near the mid-spans.

The cable tray accelerometer data is recorded on the SRB EDAS (ref. 3) systems. These data acquisition systems are mounted in the SRB's forward skirts. After the boosters are towed back to Kennedy Space Center (KSC), the EDAS systems are removed and the data is recorded and sent to the MSFC HOSC Data Reduction Center. The data was recorded on four, four-channel EDAS systems at a sampling rate of 1200 Hz, for a data bandwidth of approximately 500 Hz. The data systems collection was enabled by a "2-G turn-on" accelerometer, approximately 1.8 sec after launch, and stopped at SRB separation, approximately 2 min after launch. Synchronization among the four data systems was established by aligning the end-points of the data samples.

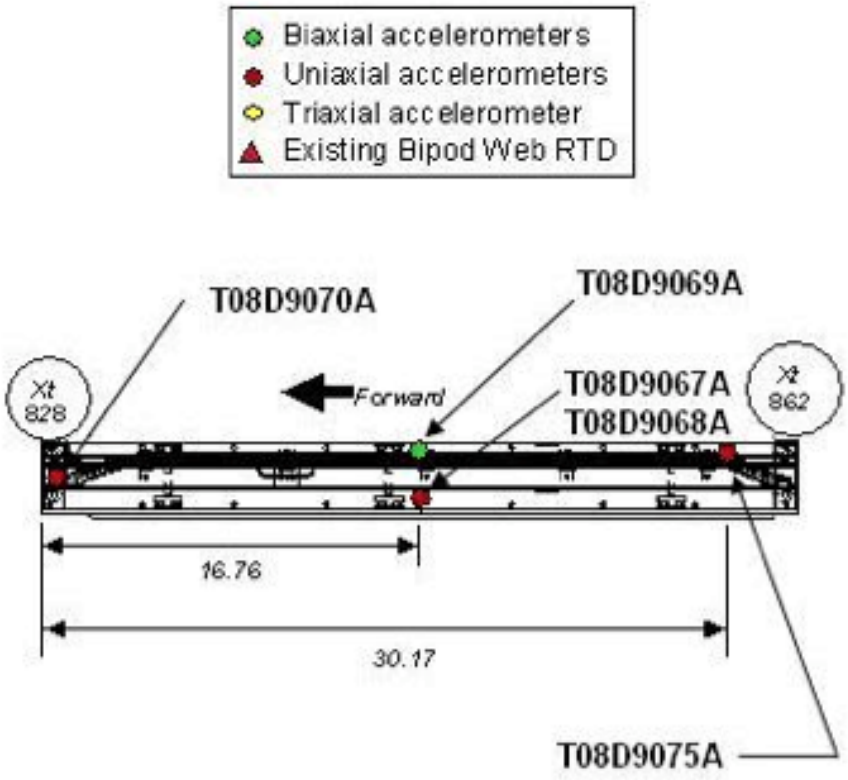


Figure 4.—$LO_2$ Cable Tray Section Accelerometer Array (NTS).

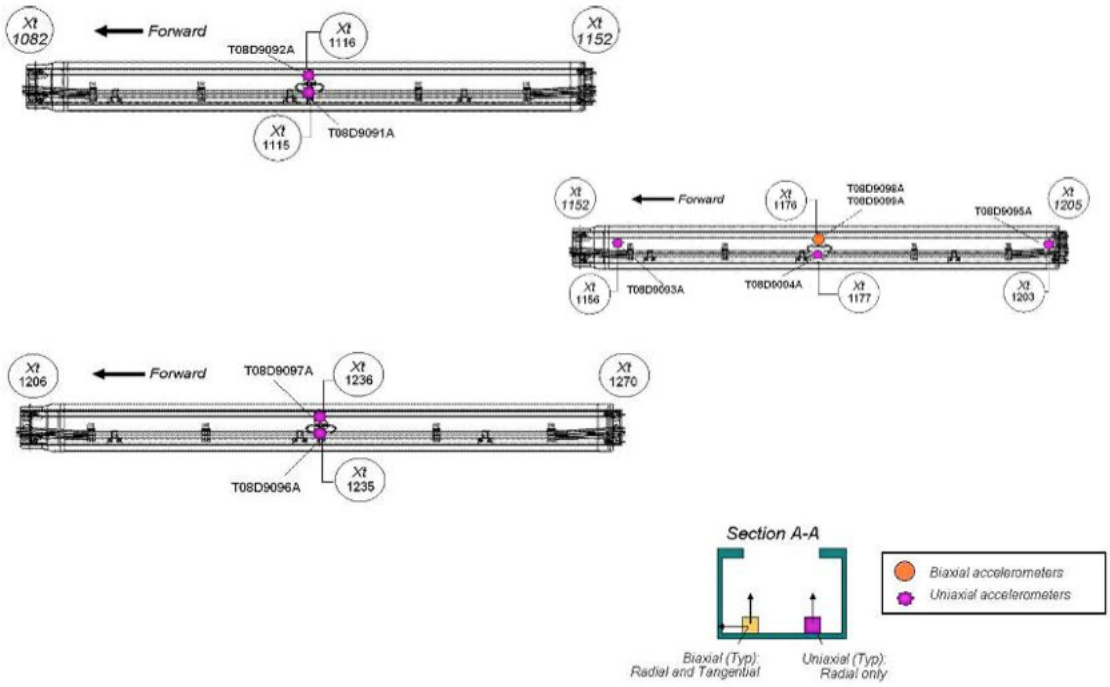


Figure 5.—Accelerometer Arrays in Three Segments of $LH_2$ Cable Tray (NTS).

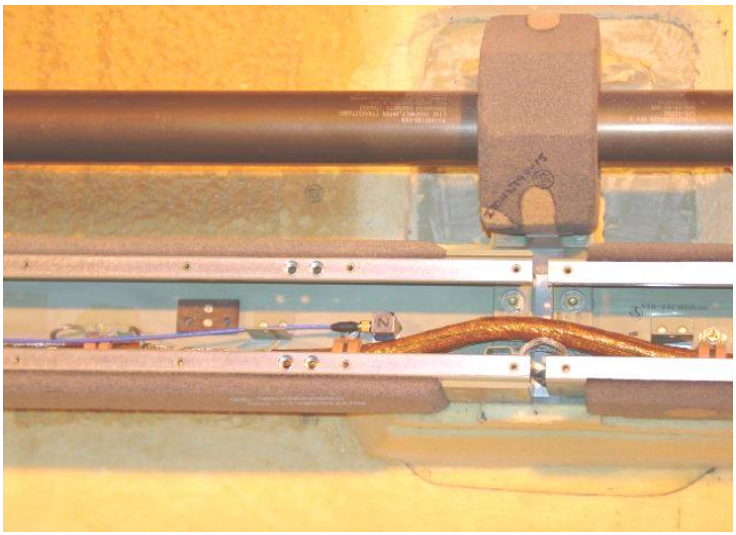

Figure 6.—Photo of Typical Accelerometer Installation.

# III. Data Analysis

A representative acceleration versus time trace from one of the tests is shown in figure 7. The first few seconds is a data system start-up transient and was ignored in the analysis. As indicated above, the data terminates at just after 120 sec, when the SRB separation process snaps the signal cables. The goal of the NESC team was to use these signals to perform advanced analyses of tray vibration velocity and displacement, modal response, and wavelet analysis of spectral/temporal responses not necessarily examined by other teams.

In general, and typical for all the measurement channels, vibration acceleration amplitude is proportional to the flight dynamic head and reaches the maximum overall signal at about 70 sec, above which the increasing vehicle velocity is countered by decreasing atmospheric density and dynamic head reduces.

Some measurement channels show a second peak in overall level at approximately 82 sec, possibly resulting from a rapid change in cross-flow during a change in vehicle attitude.

Data analyses were sought that would determine the following:

1. Overall acceleration level versus time at each sensor location
2. Frequency spectra of major vibration events
3. Correlations and phase relationships between sensor pairs
4. Assessment of resonance modes and resonance frequencies for bending and torsional vibration
5. Excitation mechanisms for primary and secondary response peaks

## A. Data De-Trend

Figure 7 shows that an initial 12-sec oscillation due to data system stabilization is present, which is un-important and ignored. The 12 to 122 sec measurement data was de-trended using a double exponential decay (short initial time constant $A^{-1}$ and long final time constant $C^{-1}$). The quasi-steady part of the acceleration was then subtracted from the total signal to obtain the fluctuating part:

$$\begin{aligned} \tilde{a}(t) &= Be^{At} + De^{Ct} + E \\ a'(t) &= a(t) - \tilde{a}(t) \end{aligned} \tag{1}$$

The fluctuating part of the signal was used for all statistical analysis. Standard software packages such as Matlab contain built-in functions for removing common steady or linear trends. However, the recorded data was not amenable to these functions. Seconds 12 to 122 of data files were least-squares curve-fit to find parameters ($A,B,C,D,E$). These are very nearly the same for all the files (illustrating the high degree of uniformity of the data acquisition channels). A graphical example of this procedure is shown in figure 8, which demonstrates a clear rise and fall in unsteady vibration level over the extent of the data acquisition period.

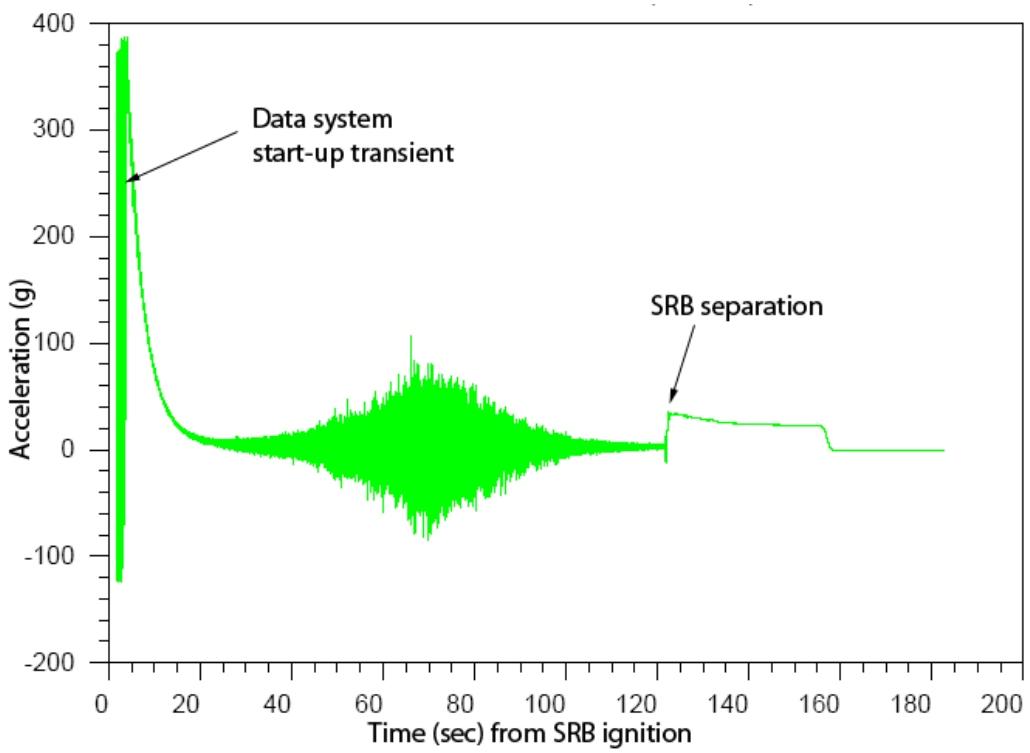


Figure 7.—Representative Acceleration Plot from EDAS System Data File.

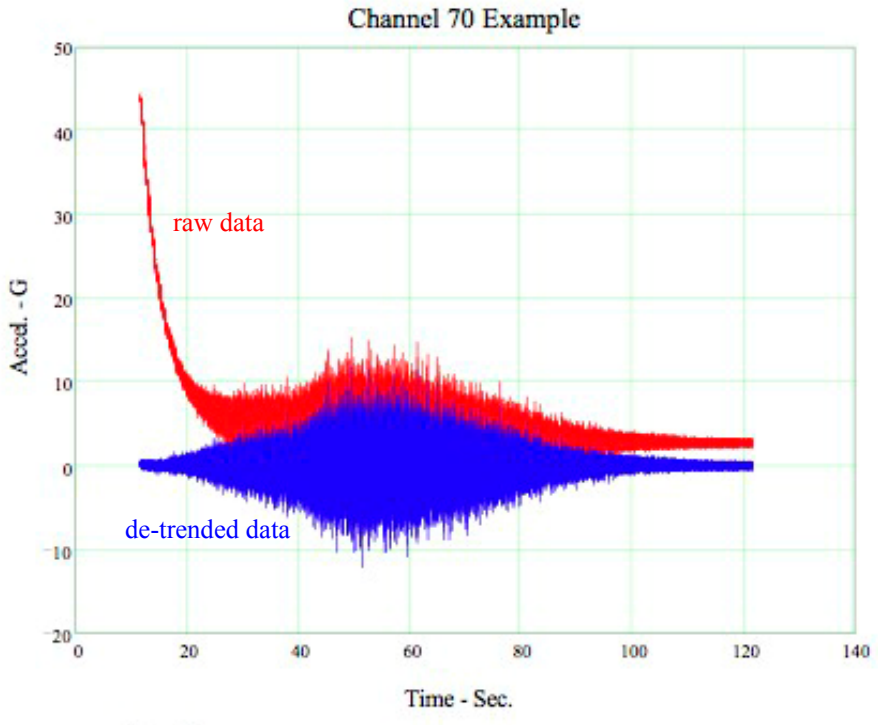


Figure 8.—Representative Unprocessed and De-Trended Acceleration Signals.

## B. Overall Signal Level Versus Time

The overall rms acceleration was computed in 1/2 sec segments for each measurement signal. Levels were compared for matching sensor locations on the three test flights. An example showing $LH_2$ sensors is presented in figure 9 (no sensors were available on the $LH_2$ PAL-On configuration). Mean acceleration characteristics between PAL-ramp off flights are similar. Figure 10 shows the accelerometer response of the $LO_2$ cable tray, for which comparison between PAL-ramp off and on flights can be made. PAL ramp removal has virtually no effect on the $LO_2$ accelerometer response.

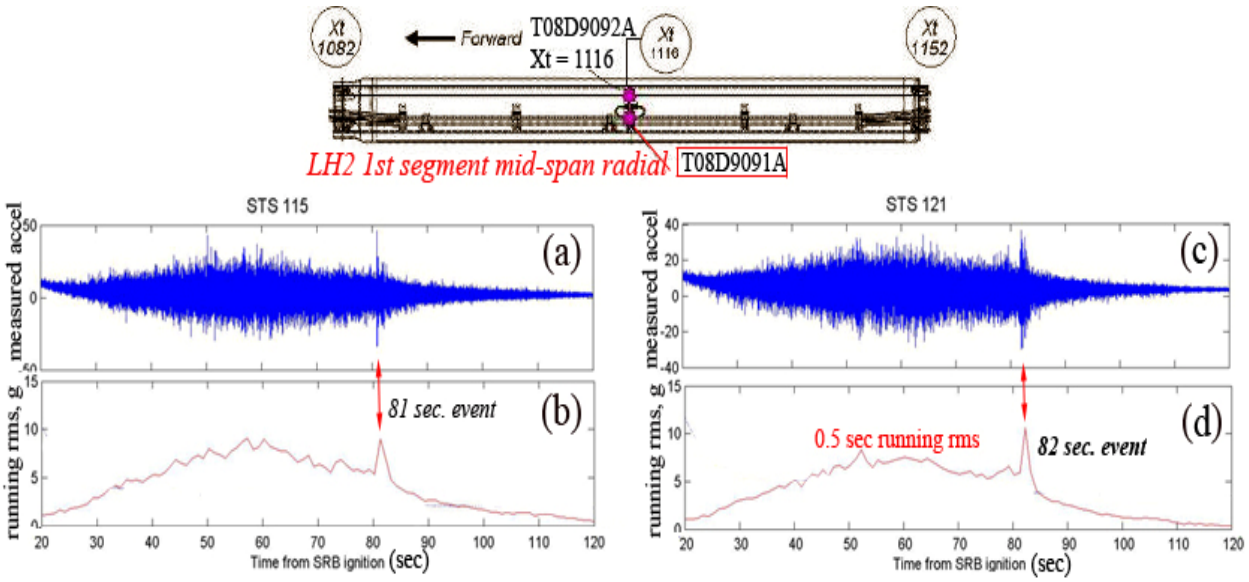


Figure 9.—Comparison of acceleration levels sensed by the mid-span, radial sensor in the first segment of the $LH_2$ Cable Tray (top sketch) in two separate flights: STS 115 (left column of plots) and STS 121(right column). (a), (c) Measured signals; (b), (d) running rms from 0.5 sec.-long data segments.

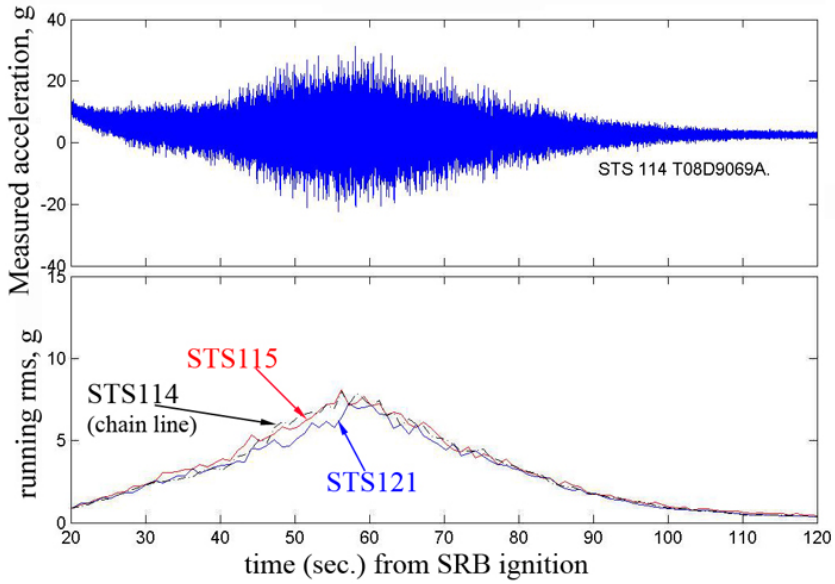


Figure 10.—Comparison of the running rms levels of accelerations sensed by mid-span sensor T08D9069A on the $LO_2$ Cable Tray from three indicated flights.

## C. Waveform Integration

In order to judge structural stresses and motion amplitudes of the cable trays, acceleration signals were integrated to produce velocity versus time and then reintegrated to produce displacement versus time plots. At each step, residual drift and offset in the signals were removed prior to integration by using the Matlab detrend function.

$$v = \int_{t1}^{t} \left[ \Delta\left( a(t1:t2) \right) \right] dt$$
$$x = \int_{t1}^{t} \left[ \Delta\left( v(t1:t2) \right) \right] dt \tag{2}$$

For the above integrations it was assumed that the initial velocity and displacement at time $t_1 = 0$ is zero. Additionally, the velocity time series was de-trended as described in the earlier section before the integration was performed. Examples of the results of these calculations are shown in figure 11. The general retention of shape is suggestive of a narrow dominant frequency band around 60 Hz for the displacement.

## D. Frequency Spectra Versus Time

Frequency spectra were evaluated by two separate techniques. First, FFT analysis was undertaken on blocks of data of varying durations. This provided both individual frequency spectra for specific times during each flight and an overall spectrographic view of each data record. Figure 12 is a spectrographic display of the radial and tangential direction acceleration spectrum results of one flight-to-flight comparison. Each subplot has two parts: the top three-dimensional color plot was obtained via Short-Time Fourier Transform of individual 0.43 sec long data segments; the time axis shows the center-time for each data segment. The bottom x-y plot shows the peak-frequencies (blue line, left scale) and the peak amplitudes (green + symbols, right scale) of the spectrogram from every time slice.

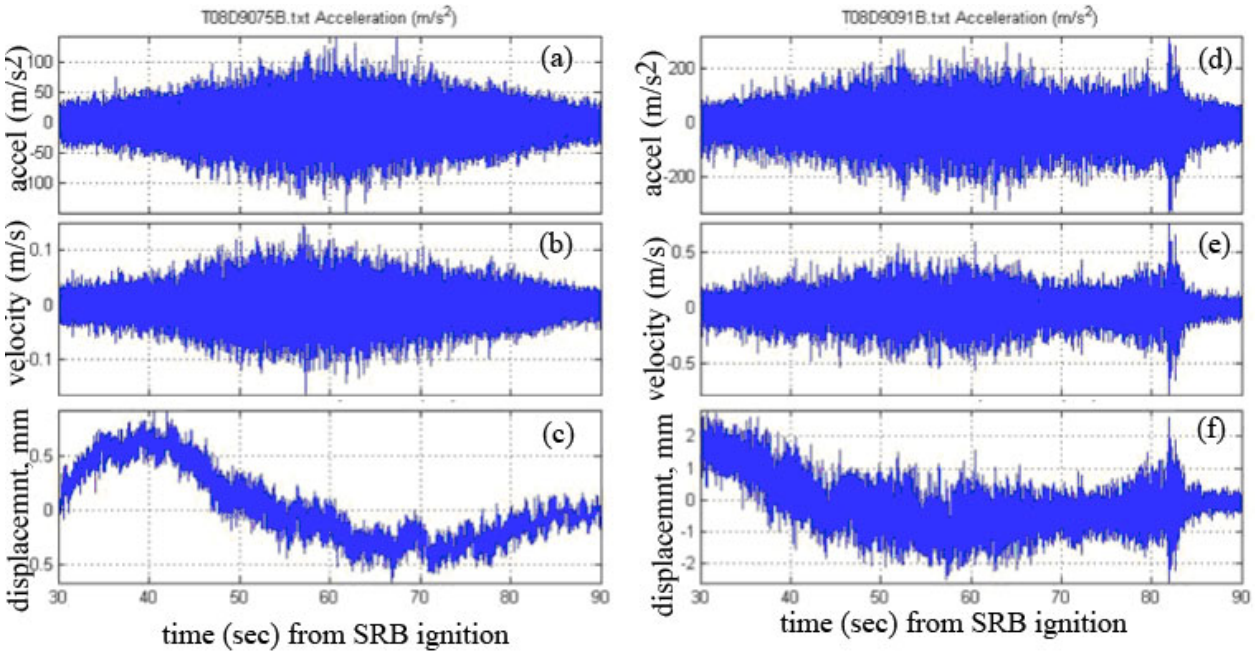


Figure 11.—Integration of accelerometer signals (a), (d) to calculate velocity (b), (e), and displacement (c), (f) time traces. The left column of plots is from a $LO_2$ sensor T08D9075B and the right from a $LH_2$ sensor T08D9091 on flight STS-121.

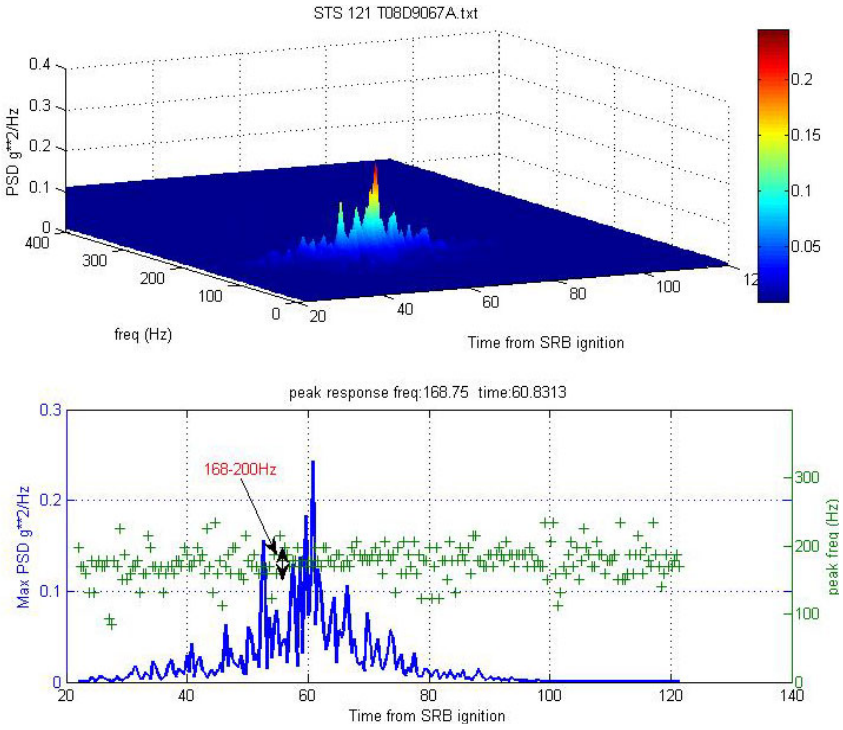


(a) ***STS-121*** radial T08D9067A, Xt = 845

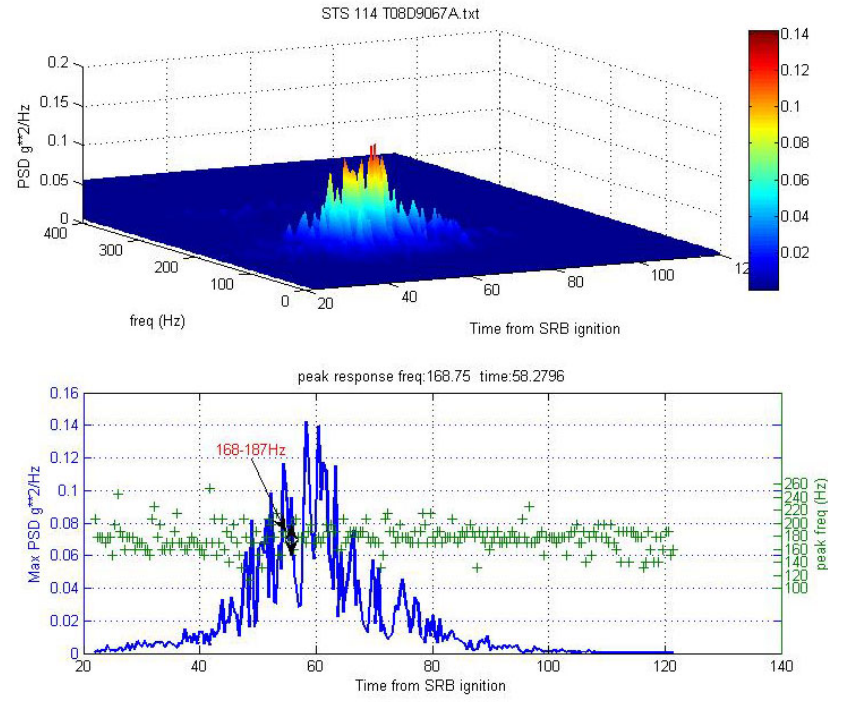


(b) ***STS-114*** radial T08D9067A, Xt = 845

Figure 12.—Frequency content comparison of the $LO_2$ cable tray accelerometer time signals from two flights. STS-121, PAL ramp removed; STS-114, PAL ramp present.

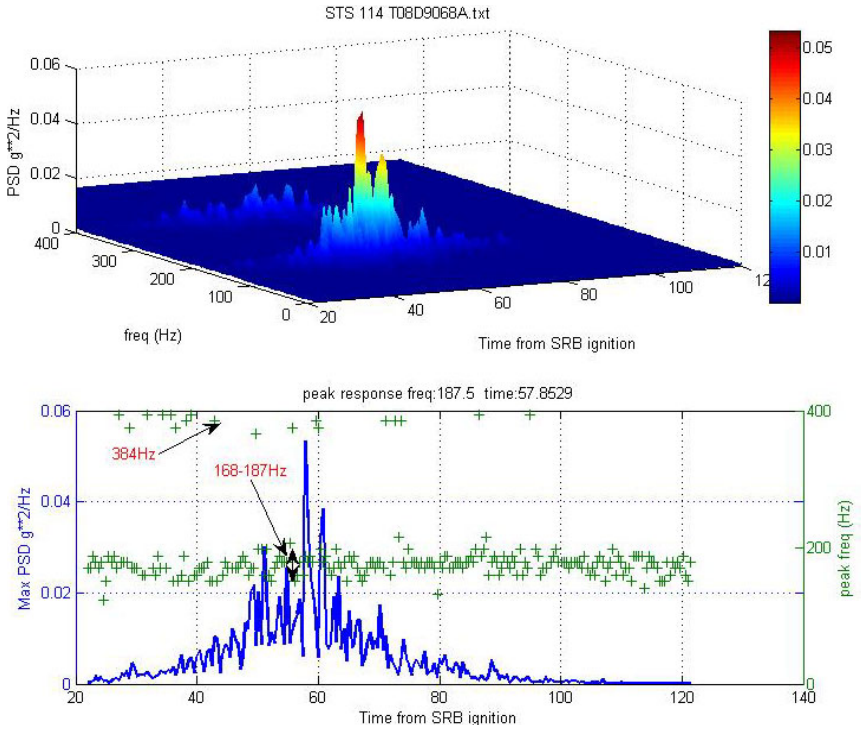


(c) ***STS-114*** tangential T08D9068A, Xt = 845

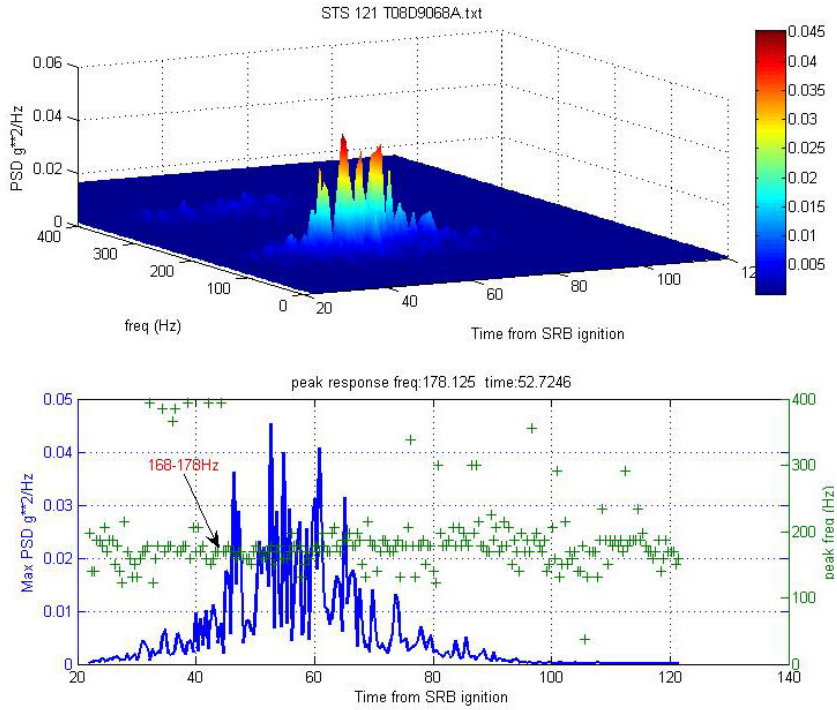


(d) ***STS-121*** tangential T08D9068A, Xt = 845

Figure 12.—Concluded. A comparison of the frequency content of the $LO_2$ cable tray accelerometer time signals from two flights. STS-121, PAL ramp removed; STS-114, PAL ramp present.

## E. Vibration Mode Analysis

Vibration sensors were located near the ends and centers of the cable tray segments. Vibration modes were investigated by comparing the amplitudes and phases of signals near spectral peaks. Signals from pairs of sensors colocated axially were used to investigate torsional motion by computing sum and difference signals in the time domain (fig. 13). Spectra were then computed for time-blocks of interest. For example, figure 14 shows a comparison of radial and torsional motions of $LH_2$ tray segment 1 for the transient signal at 81 sec. Figure 15 is a frequency-domain representation of the acceleration data. Note the strong radial spectral peak at 48 Hz and broad torsional spectral peak near 130 Hz.

Note from figure 14 that, ignoring offset due to integration of residual signal offset, the peak-to-peak radial motion of the center or the cable tray is approximately 5.5 mm at 47 to 48 Hz, whereas the torsional displacement is miniscule.

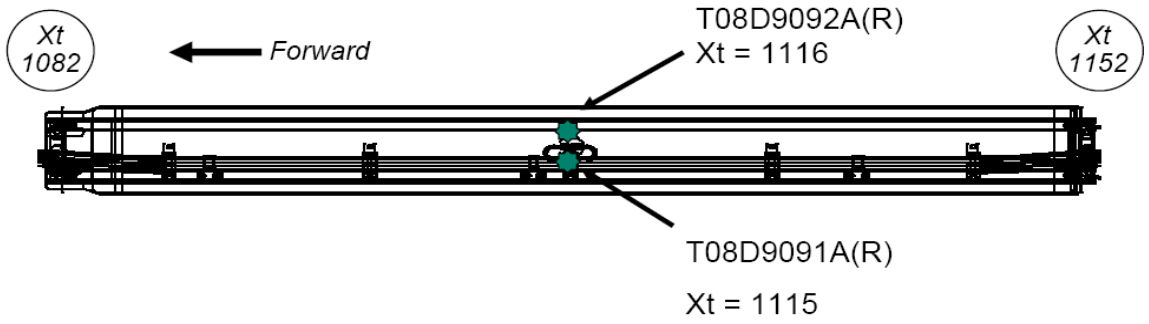


Figure 13.—Expanded View of $LH_2$ Try Segment 1 Showing Accelerometer Stations.

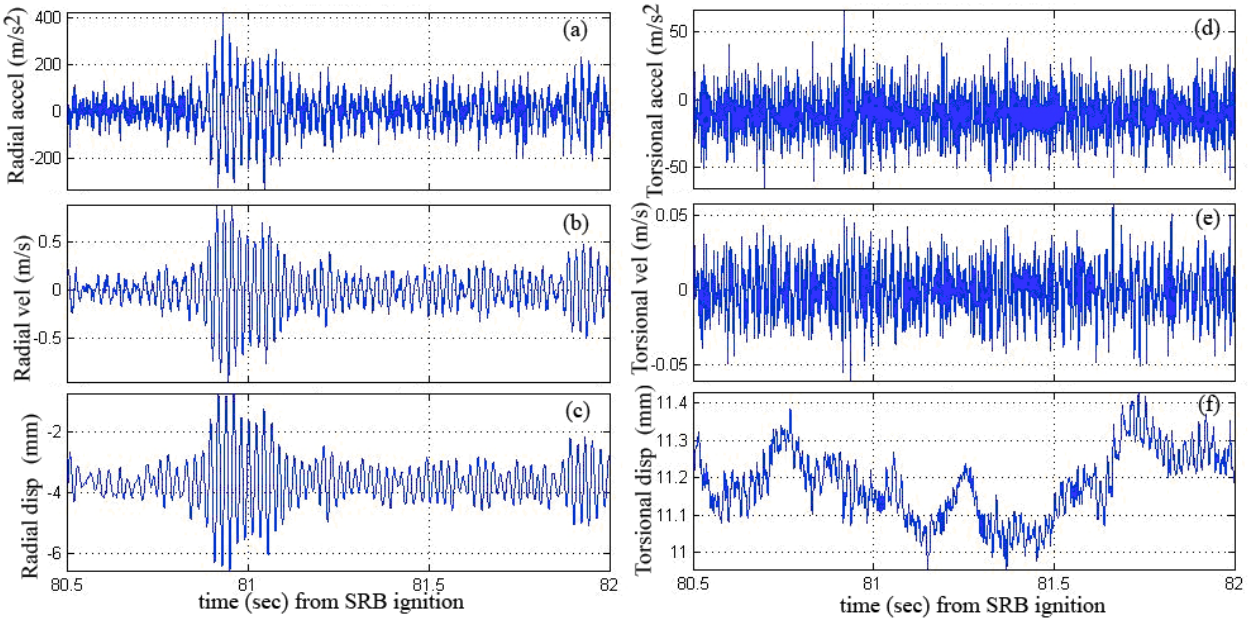


Figure 14.—Time-variation of radial (left column) and torsional (right column) acceleration, velocity and displacement calculated s near 81 sec transient on $LH_2$ Cable Tray segment 1; data from sensors T08D9091B and T08D9092B from STS-115.

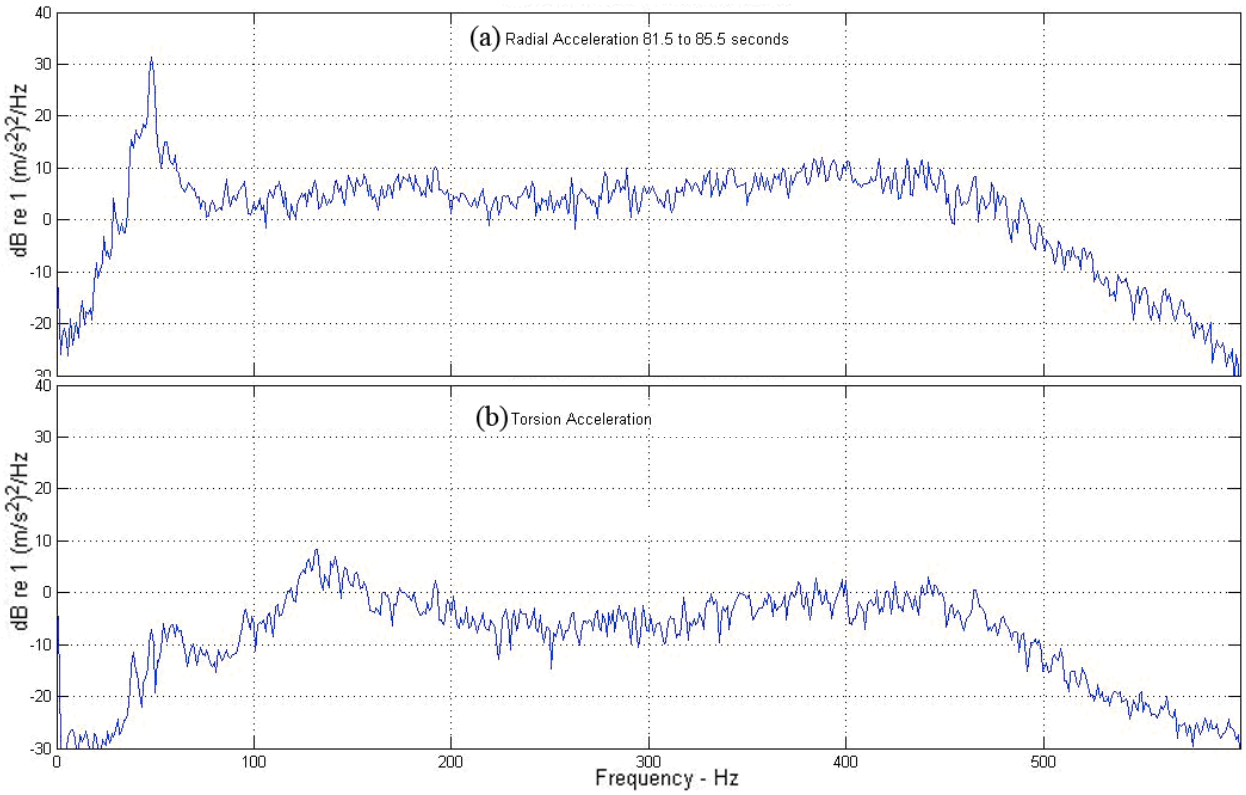


Figure 15.—Frequency Spectra of (a) radial component of the acceleration and (b) torsional component on 1st segment of $LH_2$ Cable Tray from around the 82 sec transient; data from sensors T08D9091B and T08D9092B from STS-115.

**F. Longitudinal Bending Vibration Mode From Analysis of Signal Phases**

By cross-correlating accelerometers from different locations of the cable tray, the modal frequencies and shapes of the $LO_2$, 1st span of $LH_2$ and 2nd span of $LH_2$ tray were determined. Loss of sensors and the limited number of sensors left a certain amount of uncertainty especially for the $LH_2$ tray sections. Cross-spectra and cross-correlations were calculated using the entire usable time signals between 20 and 120 sec. Primary response in 170 to 180 Hz and a secondary at 125 Hz are in phase (~ 0° phase). Since the signals from the forward, mid-span and rear sensors are all in phase for the 125 Hz and 170 to 180 Hz ranges, the motion is a plunging mode where the entire span appears to move radially up and down in phase. Representative results are shown in figures 16 and 17.

**G. Wavelet Transform Analysis**

The 80 to 84 sec anomaly in the $LH_2$ tray response was analyzed using Wavelet analysis. The issue with the statistical analysis of a transient event (that includes any flight data from rocket vehicles) is the nonstationary nature of the time signal. Calculation of moments, Fourier Transform etc requires stationary data, and may lead to large uncertainty when applied to the current accelerometer signals. The Short-time Fourier transform provides a suitable means but masks fast-changing events. The complex and rapidly changing vibration pattern around the time of the "82-sec event" suggested a need for a more detailed analysis than a simple spectrograph could provide. Wavelet transform analysis (ref. 4) was used to examine the time-frequency-amplitude/phase responses. This method offers an improved optimization of frequency and time resolution over the measurement bandwidth relative to usual PSD or spectrographic technique, at the expense of being more computationally intense.

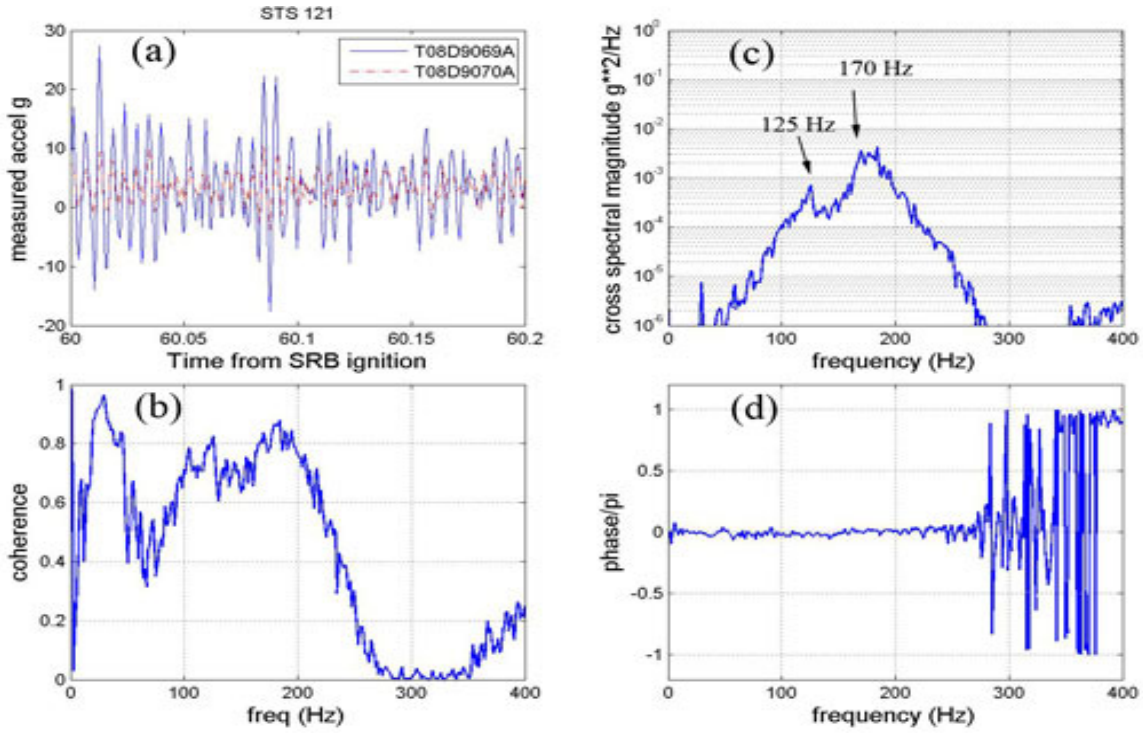


Figure 16.—(a) Part of the time signal from two radial accelerometers: forward T08D9070A and mid-span T08D9069A on $LO_2$ Cable Tray on STS121. (b) Coherence spectrum (c) cross-spectrum magnitude (d) cross-spectrum phase.

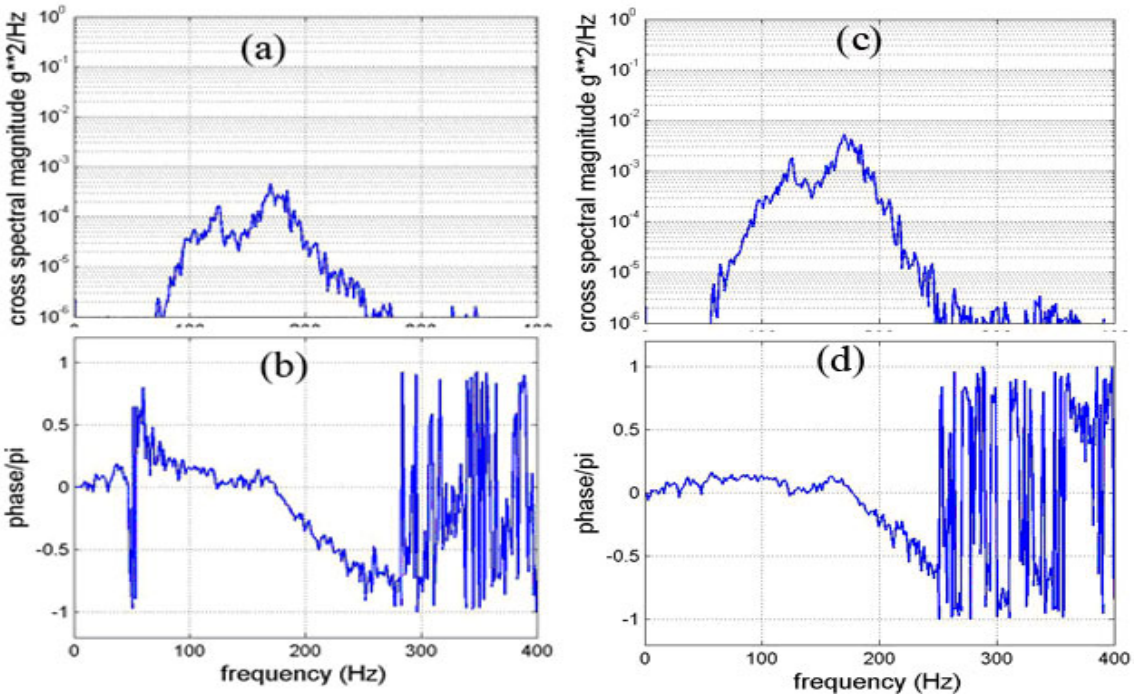


Figure 17.—Correlation plots demonstrating frequency and modal content of $LO_2$ tray in STS121 flight.(a), (b) Cross-spectrum and phase between forward T08D9070A and rear T08D9075A sensors (c), (d) same between mid-span T08D9069A and rear T08D9075A sensors.

Well-defined Gaussian resolution of frequency and time are achieved with the Morlet wavelet function. By definition: a complex Morlet wavelet is

$$\psi(x) = \frac{1}{\sqrt{\pi F_b}} e^{2\pi i F_c x} e^{-\left(x^2/F_b\right)} \tag{3}$$

depending on two parameters: $F_b$ is a bandwidth parameter; $F_c$ is a wavelet center frequency. Four-cycle and eight-cycle complex Morlet wavelets were used for this analysis. The four-cycle version is illustrated graphically in figure 18.

The continuous wavelet transformation at scale $S$ is equivalent to cross-correlating scaled copies of this function with the test signal, resulting in optimized or uniform time-bandwidth product signal decomposition. In this case, the center frequency of the wavelet is the sampling rate times the inverse of the wavelet scale and the bandwidth is approximately center frequency times the inverse of the bandwidth parameter (4 or 8).

$$\Psi(a,t) = \int_R a'(\tau) \frac{1}{\sqrt{a}} \psi_{cmor}\left(\frac{t-\tau}{a}\right) d\tau \tag{4}$$

The continuous complex wavelet transformation was used to provide a representation of the time history of signal frequency components in the time just prior to transient events identified in the overall signal. The scale factor a of the wavelet transform is converted to frequency via the use of the center frequency $F_c$ and the sampling rate 1/T, where T is the time interval between the adjacent samples via the following:

$$f_{cmor} = \frac{F_c}{a\mathrm{T}} \tag{5}$$

## H. Investigation of Transients

Effort was concentrated on understanding mechanisms causing observed $LH_2$ tray transient vibration at approximately 80 to 82 sec and repeatable for the two flights with the $LH_2$ tray instrument. Figure 19 is an example of the results that were achieved by the wavelet analysis approach. The time leading up to the transient peak is characterized by quasi-steady noise just below 50 Hz, accompanied by a linearly increasing-frequency signal that starts at about 22 Hz at 73 sec. This response may be the result of changing flow angle over a protrusion as vehicle attitude shifts. The strongest transient, which is seen in the conventional analysis, occurs near the intersection of the steady and rising-frequency signals, then decays rapidly.

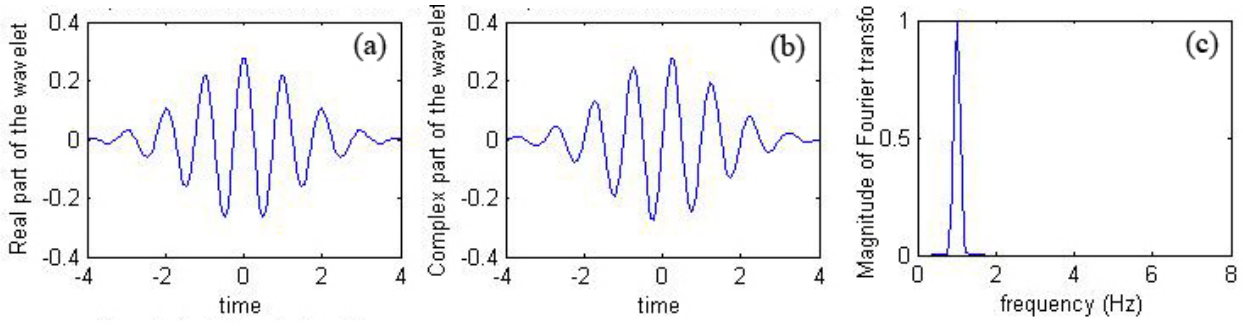


Figure 18.—Parts of Complex Morlet Wavelets (a) Real and (b) imaginary parts of a complex Morlet Wavelet and, (c) its Fourier transform. The center frequency $F_c$ = 1, and bandwidth $F_b$ = 4.

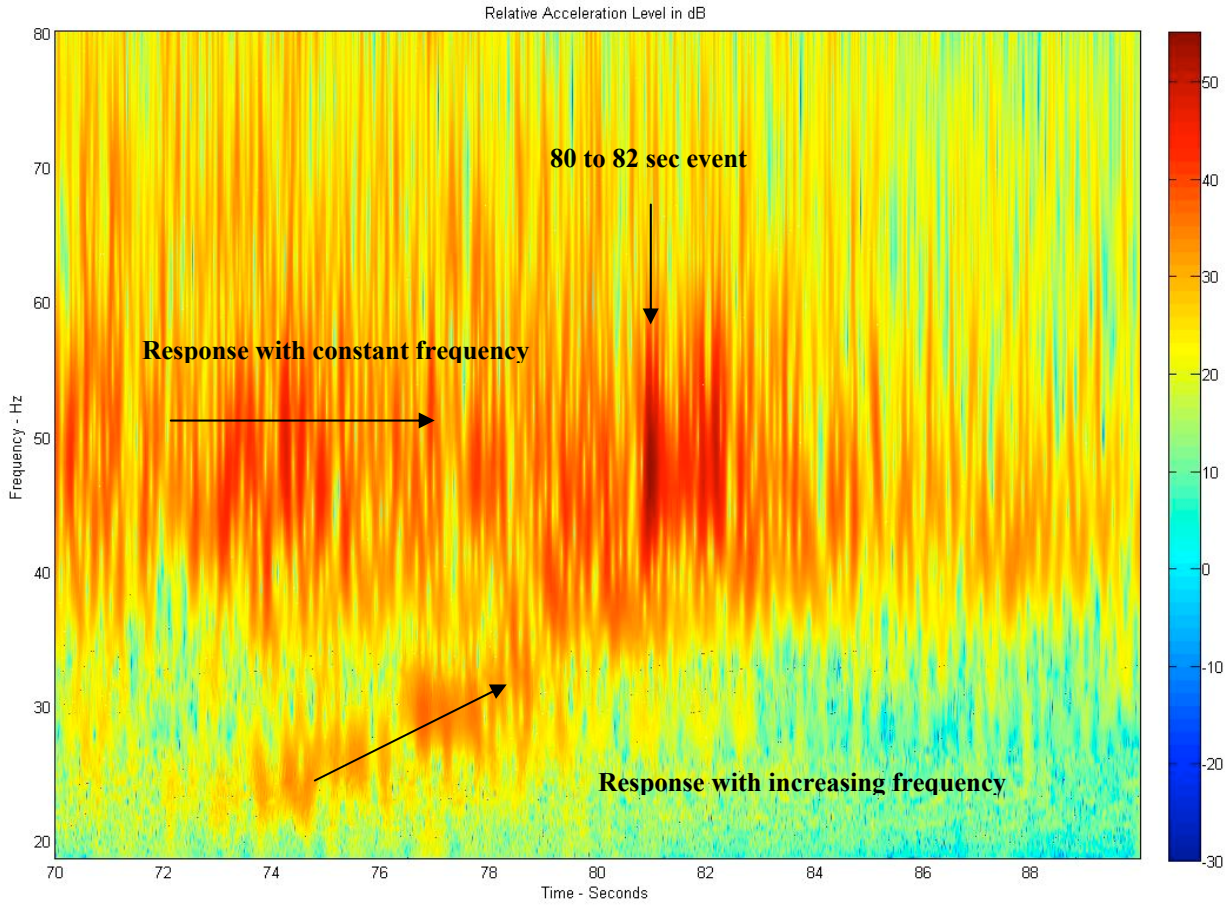


Figure 19.—Amplitude of the complex wavelet transform (dB) calculated from the radial component of acceleration of the 1st segment of the $LH_2$ Cable Tray in STS-121 flight. Data segment from near the 82 sec event.

# IV. Conclusions

One segment of the $LO_2$ Cable Tray and three segments of the $LH_2$ Cable Tray were instrumented with accelerometers in three different Space Shuttle flights to access structural integrity during ascent through the atmosphere, and to establish the effect of the removal of the PAL ramps. For the most part the vibratory response was found to be proportional to the flight dynamic pressure (q), with the max-response appearing at the highest dynamic pressure from around 60 sec into the flight. This trend was disrupted by a spurious event around 80 to 84 sec where an anomalous increase in response from some $LH_2$ sensors were noticed in spite of a falling dynamic pressure.

Integration of the accelerometer signals produced time variation of velocity and displacement. Additionally, signals from two radial accelerometers placed at the same cross-sectional plane of the Tray were added and subtracted to determine the radial and torsional components of acceleration. These components of acceleration were then integrated to calculate displacements in the individual directions. A closer look into such time signals showed short bursts of periodic responses at the dominant structural frequencies. The signal was characteristic of a forced response under high random fluctuations that did not lead to any flutter. Also, the damping of the cable tray was significant; this caused decay of the periodic responses. Typically, the radial displacement at max q was between 2 to 5 mm; the torsional displacement was an order of magnitude lower than the radial component. Displacement values at the maximum dynamic pressure were deemed to be within the expected range from prior modeling and testing efforts.

In order to determine the frequencies and modal content of the vibratory motion, the time signals were segmented into small parts corresponding to different intervals of flight, and Short-Time Fourier Transform was performed on individual segments. Additionally, cross-spectral magnitude and phase were calculated from various sensors placed within the same segments of the Cable Tray. Such analysis for the $LO_2$ Cable Tray found responses

primarily at 170 to 180 Hz, and a secondary response at 125 Hz. Since signals from the forward, mid-span and rear sensors were all found to be in phase for both of these frequencies the motions were attributed to plunging modes where the entire span moved radially up and down in phase. Similar analyses for the segments of $LH_2$ Cable Tray also confirmed the radial plunging modes as the most dominant, followed by the lateral (inboard-outboard) modes as the next dominant modes of vibration. The frequencies showed reasonable agreement with those measured during ground vibration tests.

The 80 to 84 sec anomaly in the $LH_2$ tray response was further analyzed using wavelet analysis. As opposed to statistical methods that require stationary data, wavelet analysis can be applied to fast transient events. It was observed that an increasing frequency phenomenon started from around 74 sec into the flight. The phenomenon reached the plunging mode of various $LH_2$ tray segments between 80 to 84 sec, and led to the large structural response. The exact cause for this event could not be identified; although it was conjectured to be a vortex shedding phenomenon that coincided with the change in the vehicle angle-of-attack. The very short duration of this event deemed to have little impact on the life cycle of the Cable Tray.

The effect of the removal of the PAL ramp was accessed by analyzing data from STS-114 (with PAL), STS-121(no PAL, low q flight) and STS-115 (no PAL, high-q flight). The frequencies and amplitudes of the response were found to nearly identical (except for the minor differences due to different flight q). This showed that the PAL ramp removal has no effect on the vibratory response of the $LO_2$ Cable Tray. The ramification of this observation is either $LO_2$ Tray does not see any shock-induced cross-flow (the original reason for the PAL ramps), or the buffet part of the dynamic load is insignificant compared to the transmitted vibratory load to the Tray segments.

# References


1. "Aeroelastic Response and Protection of Space Shuttle External Tank Cable Trays," J.W. Edwards, D.F. Keller, D.M. Schuster, D.J. Piatak, R.D. Rausch, R.E Bartels, T.G. Ivanco, S.R. Cole, and C.V. Spain; AIAA–2005–3627, 41st AIAA/ASME/SAE/ASEE Joint Propulsion Conference and Exhibit, 10–13 July 2005, Tucson, Arizona.
2. "Estimation of the Unsteady Aerodynamic Load on Space Shuttle External Tank Protuberances From a Component Wind Tunnel Test," J. Panda, F.W. Martin, and D.L. Sutliff, AIAA–2008–0232, 46th AIAA Aero Sciences Conference, January 7–11th, 2008, Reno Nevada.
3. "ET Project—Instrumentation Program and Components and Flight List—DFI" MMC-ET-SE09-07 Rev C February 2006, Contact NAS8-00016 WBS 4.6.1.7.
4. *Wavelet Toolbox for Use With Matlab*, M. Misti, Y., Misti, G., Oppenheim, J.-M. Poggi, The MathWorks, March, 2006.

| REPORT DOCUMENTATION PAGE | | | Form Approved OMB No. 0704-0188 |
|---|---|---|---|



| 1. REPORT DATE *(DD-MM-YYYY)* | 2. REPORT TYPE | 3. DATES COVERED *(From - To)* |
|---|---|---|
| 01-03-2008 | Technical Memorandum | |

**4. TITLE AND SUBTITLE**
Vibration Analysis of the Space Shuttle External Tank Cable Tray Flight Data With and Without PAL Ramp

**5a. CONTRACT NUMBER**

**5b. GRANT NUMBER**

**5c. PROGRAM ELEMENT NUMBER**

**6. AUTHOR(S)**
Walker, Bruce, E.; Panda, Jayanta; Sutliff, Daniel, L.

**5d. PROJECT NUMBER**

**5e. TASK NUMBER**

**5f. WORK UNIT NUMBER**
WBS 510.505.04.03.01

**7. PERFORMING ORGANIZATION NAME(S) AND ADDRESS(ES)**
National Aeronautics and Space Administration
John H. Glenn Research Center at Lewis Field
Cleveland, Ohio 44135-3191

**8. PERFORMING ORGANIZATION REPORT NUMBER**
E-16379

**9. SPONSORING/MONITORING AGENCY NAME(S) AND ADDRESS(ES)**
National Aeronautics and Space Administration
Washington, DC 20546-0001

**10. SPONSORING/MONITORS ACRONYM(S)**
NASA

**11. SPONSORING/MONITORING REPORT NUMBER**
NASA/TM-2008-215156; AIAA-2008-312

**12. DISTRIBUTION/AVAILABILITY STATEMENT**
Unclassified-Unlimited
Subject Category: 18
Available electronically at http://gltrs.grc.nasa.gov
This publication is available from the NASA Center for AeroSpace Information, 301-621-0390

**13. SUPPLEMENTARY NOTES**

**14. ABSTRACT**
External Tank Cable Tray vibration data for three successive Space Shuttle flights were analyzed to assess response to buffet and the effect of removal of the Protuberance Air Loads (PAL) ramp. Waveform integration, spectral analysis, cross-correlation analysis and wavelet analysis were employed to estimate vibration modes and temporal development of vibration motion from a sparse array of accelerometers and an on-board system that acquired 16 channels of data for approximately the first 2 min of each flight. The flight data indicated that PAL ramp removal had minimal effect on the fluctuating loads on the cable tray. The measured vibration frequencies and modes agreed well with predicted structural response.

**15. SUBJECT TERMS**
Space shuttle; Flight data; Dymanic loads analysis

| 16. SECURITY CLASSIFICATION OF: | | | 17. LIMITATION OF ABSTRACT | 18. NUMBER OF PAGES | 19a. NAME OF RESPONSIBLE PERSON |
|---|---|---|---|---|---|
| a. REPORT | b. ABSTRACT | c. THIS PAGE | | | STI Help Desk (email:help@sti.nasa.gov) |
| U | U | U | UU | 23 | 19b. TELEPHONE NUMBER *(include area code)* 301-621-0390 |